

Supporting Information

Development of a near infrared Au-Ag bimetallic nanocluster for ultrasensitive detection of toxic Pb²⁺ ions *in vitro* and inside cells

Achinta Sannigrahi^{1,#}, Sourav Chowdhury^{1,2,#}, Indrani Nandi^{1,3}, Dwipanjan Sanyal¹, Sayantani Chall^{1,*} and Krishnananda Chattopadhyay^{1,3,*}

¹**Structural Biology & Bio-Informatics Division, CSIR-Indian Institute of Chemical Biology, 4, Raja S. C. Mallick Road, Kolkata 700032, India.**

²**Department of Chemistry and Chemical Biology, Harvard University, 12, Oxford Street, Cambridge Massachusetts, USA.**

³**Academy of Scientific and Innovative Research (AcSIR), Ghaziabad 201002, India**

***Corresponding Author Email: krish@iicb.res.in, sayantani.chall@yahoo.com**

contributed equally.

Table S1. Volume and molar ratio of Au³⁺ and Ag⁺ used for the synthesis of Au-Ag@BSA NCs.

Au:Ag	Volume ratio (ml)	Molar ratio (M)
	2.0:0.5	3.6:0.8
	1.5:1.0	2.7:1.6
	1.25:1.25	2.3:2.0
	1.0:1.5	1.8:2.4
	0.5:2.0	0.9:3.1

Table S2. Time resolved study of Au-Ag@BSA NCs with simultaneous variation of Au and Ag molar ratios.

[AuCl ₄ ⁻] (mM)	[Ag ⁺] (mM)	λ_{ems}	τ_1 (ns)	τ_2 (ns)	τ_{av} (ns)	χ^2
4.5	0	680	1.74	260	211	1.08
3.6	0.8	665	1.48	157	133	1.13
2.7	1.6	703	5.64	112	100	1.16
2.3	2.0	718	1.04	98.6	14.2	1.25
1.8	2.3	766	1.37	116	11	1.16
0.9	3.1	815	0.9	64	2.5	1.04

Table S3. Different sensors for the detection of contaminants (toxic ions).

Sensing Probes	Contaminant	LOD	Ref.
Au NP	Pb ²⁺	100 nM	1
Au NP	Pb ²⁺	3 nM	2
Au NC	Hg ²⁺	0.1 nM	3
Au NC	Fe ³⁺	5.4 μM	4
Au NC-QD conjugate	Hg ²⁺	9 nM	5
Au NP-Graphene Oxide conjugate	Pb ²⁺	0.1 nM	6
Au NC	CN ⁻	2 nM	7
Au nanofilm	Pb ²⁺	0.1 μmolL ⁻¹	8
DNAzyme-Au NP hybrid	Pb ²⁺	0.028 nM	9
Au NC	Pb ²⁺	10 nM	10
Au-Ag NC	Pb ²⁺	96.02 nM	Present work

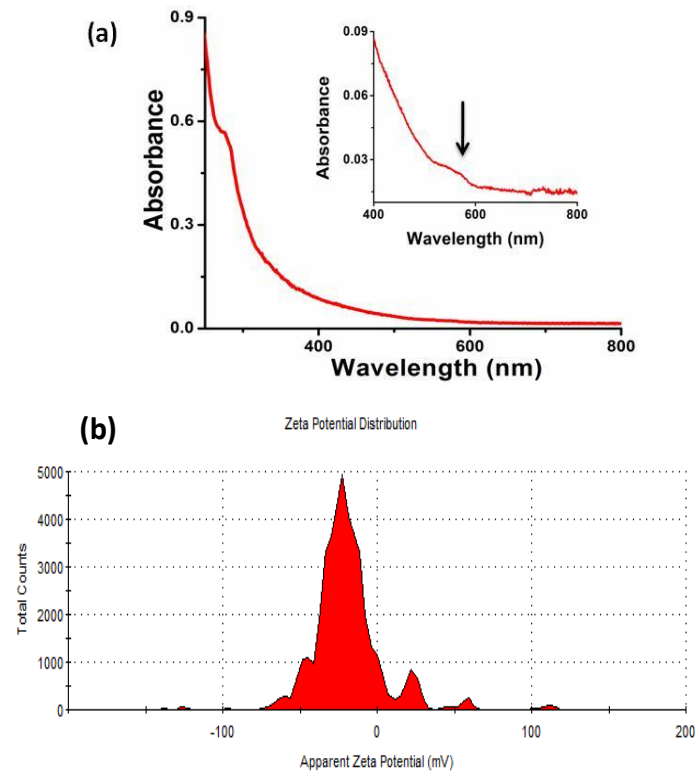


Figure S1. (a) Absorption spectra of Au-Ag@BSA NCs where Au-Ag molar ratio was 2.3:2, inset shows broad shoulder due to the incorporation of Ag (zoomed in from Figure S1a); (b) Zeta potential of Au-Ag@BSA NCs.

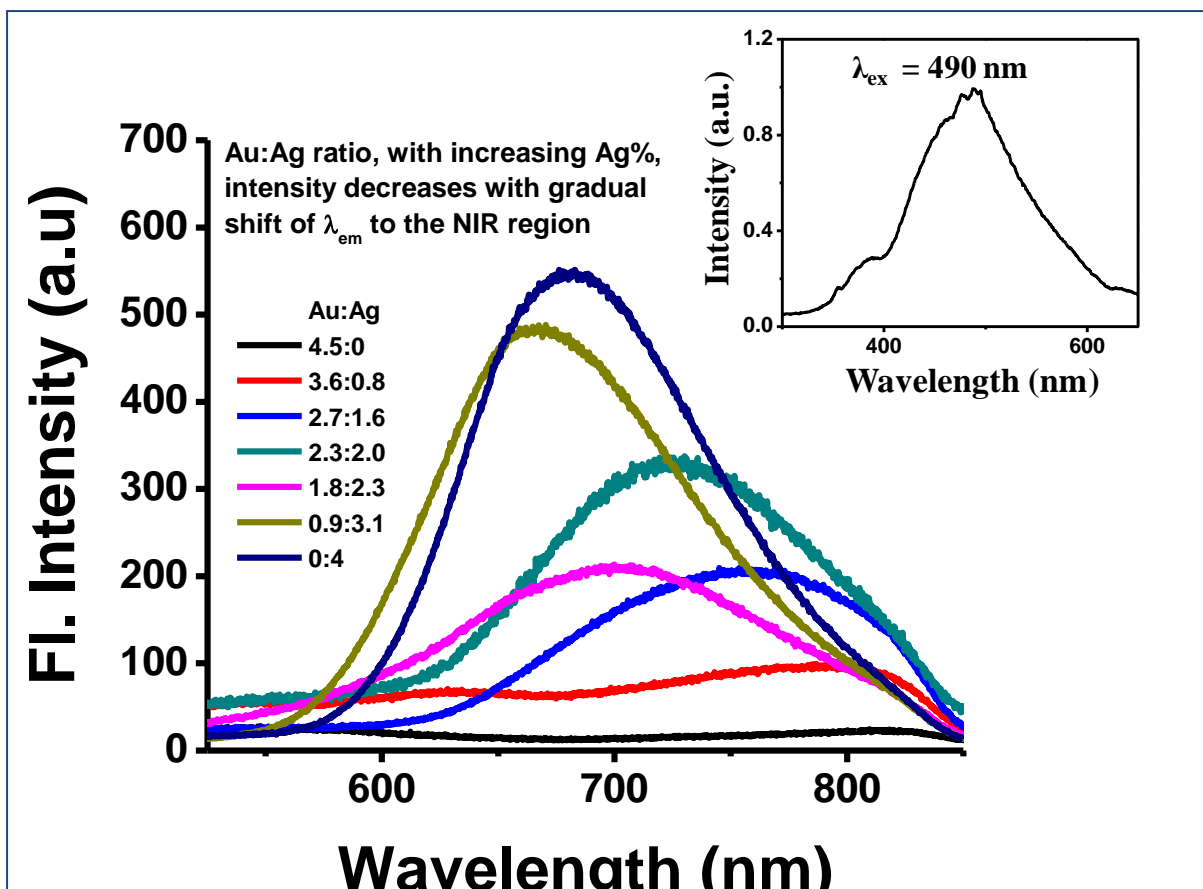


Figure S2. Decrease of fluorescence Intensity of Au-Ag@BSA NCs with increasing concentration of Ag, inset: excitation spectrum of Au-Ag@BSA NCs.

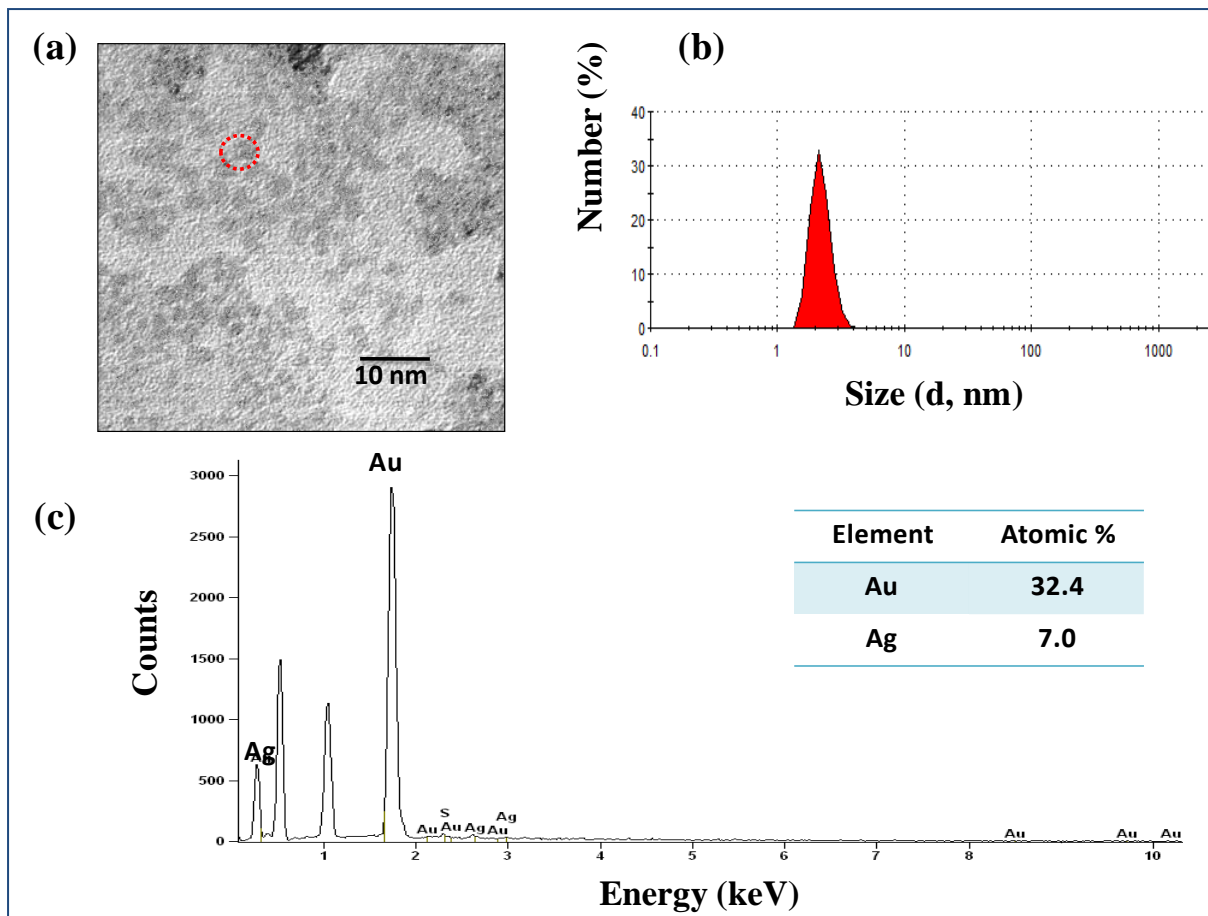


Figure S3. (a) TEM image of as prepared Au-Ag@BSA NCs, Scale bar was 10 nm; (b) DLS size distribution of Au-Ag@BSA NCs showed the existence of higher population of particles ~2 nm in diameter; (c) EDAX spectrum showed the composition and apparent atomic ratio of Au and Ag in Au-Ag@BSA NCs. Inset table showed the elemental composition (Au/Ag) of Au-Ag@BSA NCs.

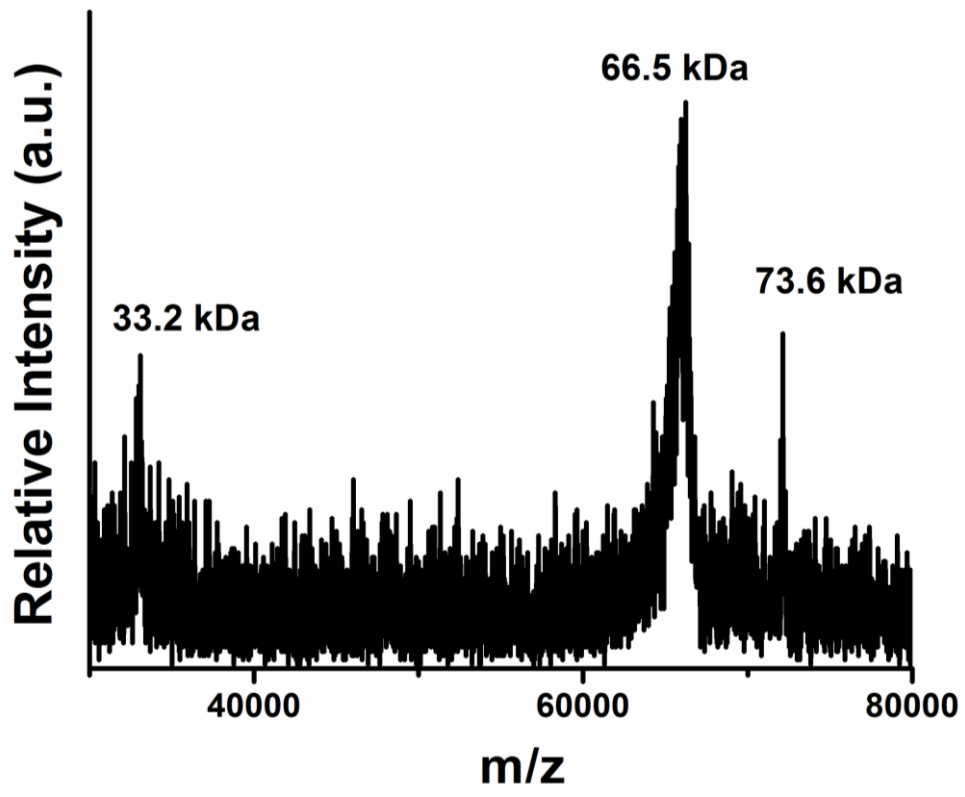


Figure S4. MALDI mass spectrum of as-prepared Au-Ag@BSA NC.

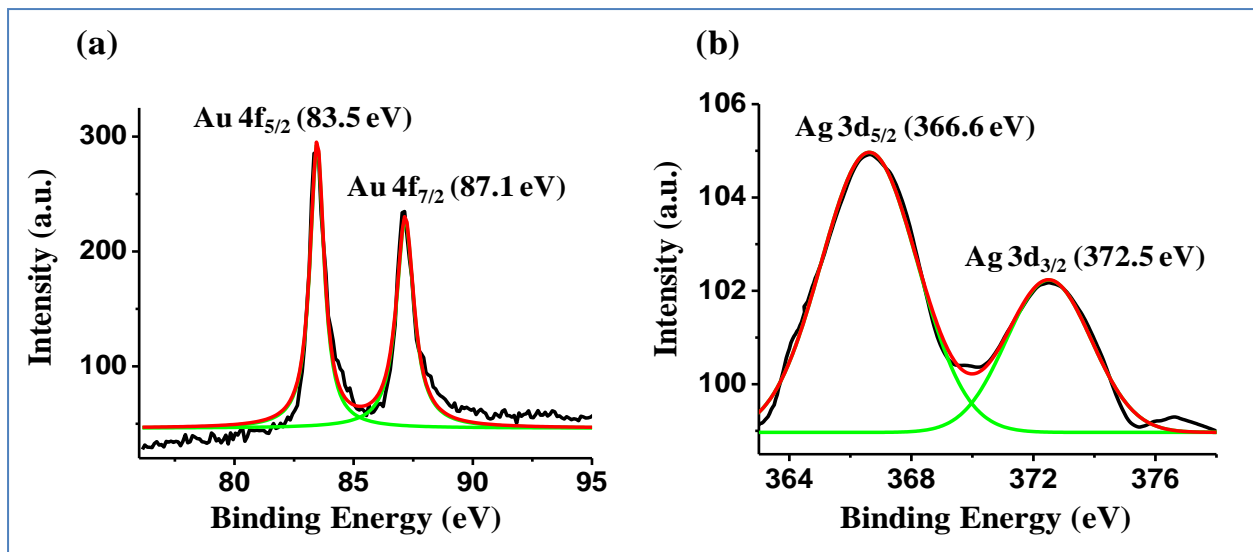


Figure S5. X-ray photoelectron spectra (XPS) of (a) Au 4f and (b) Ag 3d of Au-Ag@BSA NCs.

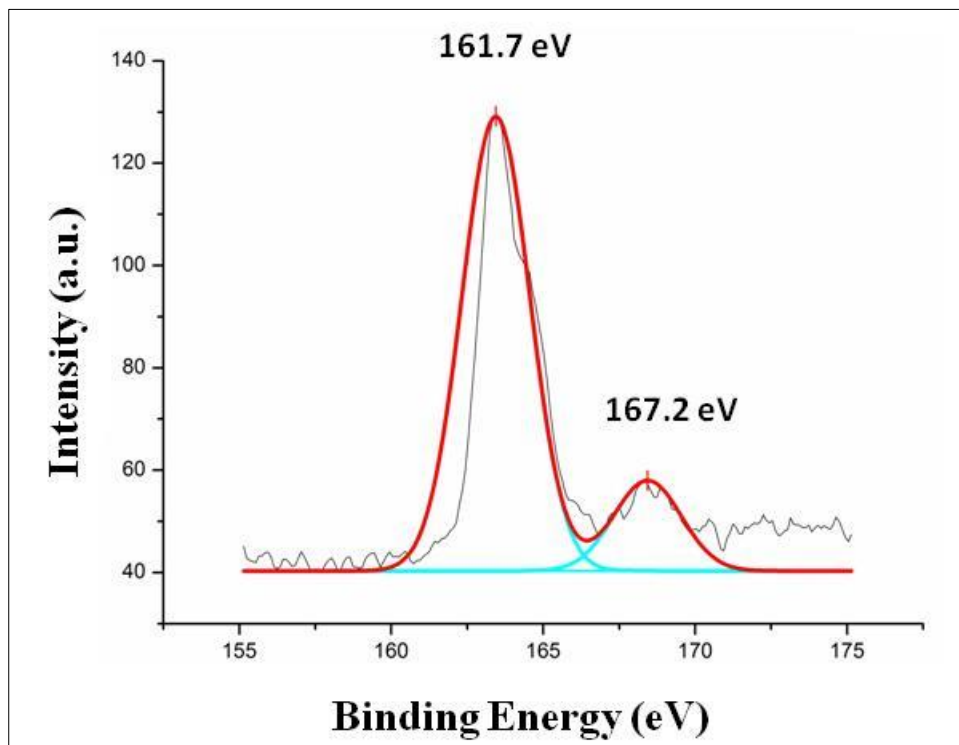


Figure S6. X-ray photoelectron spectra of S 2p states.

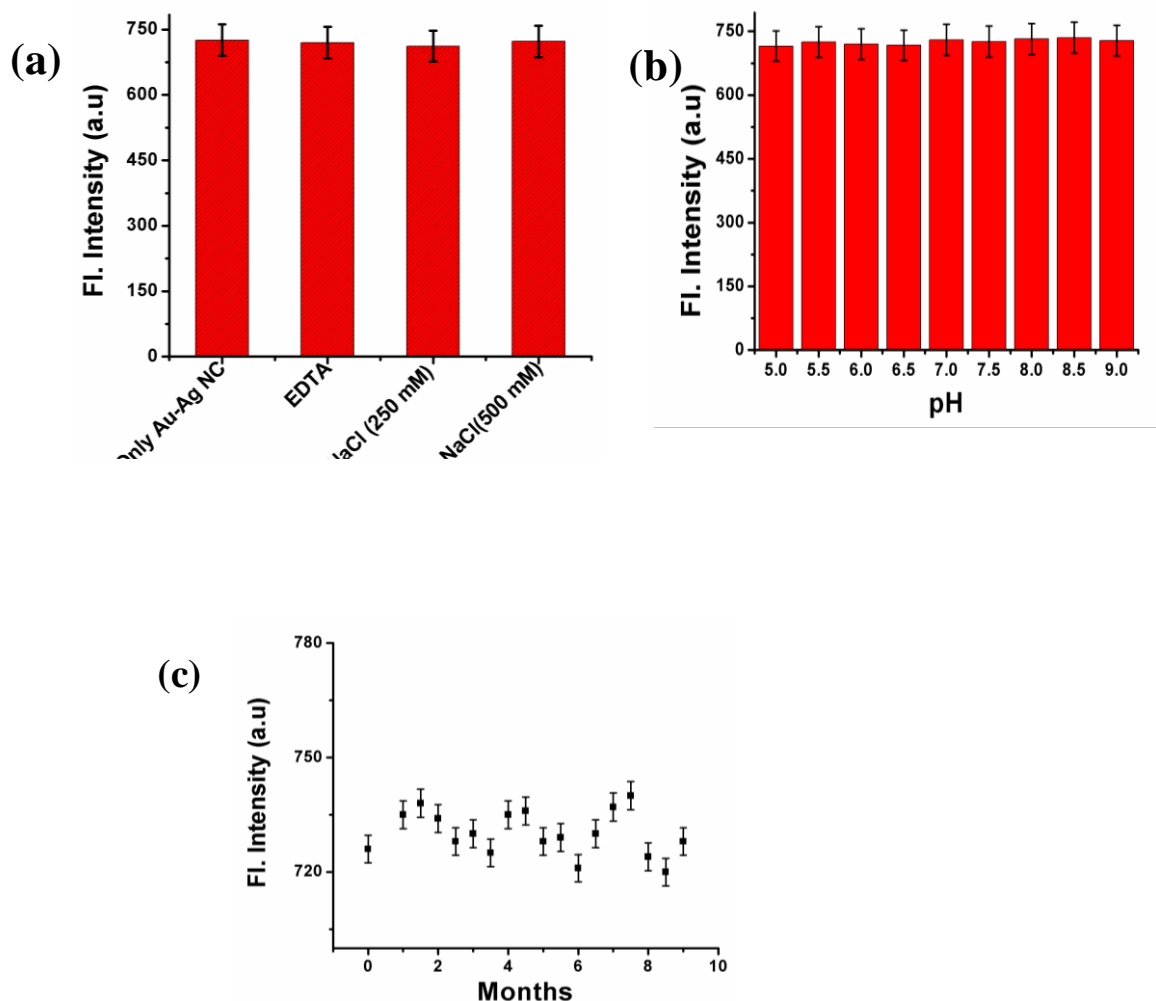


Figure S7. Fluorescence Stability of the as prepared Au-Ag@BSA nanocluster in presence of (a) EDTA and NaCl; (b) at different pH; (c) Au-Ag@BSA NCs fluorescence stability with time.

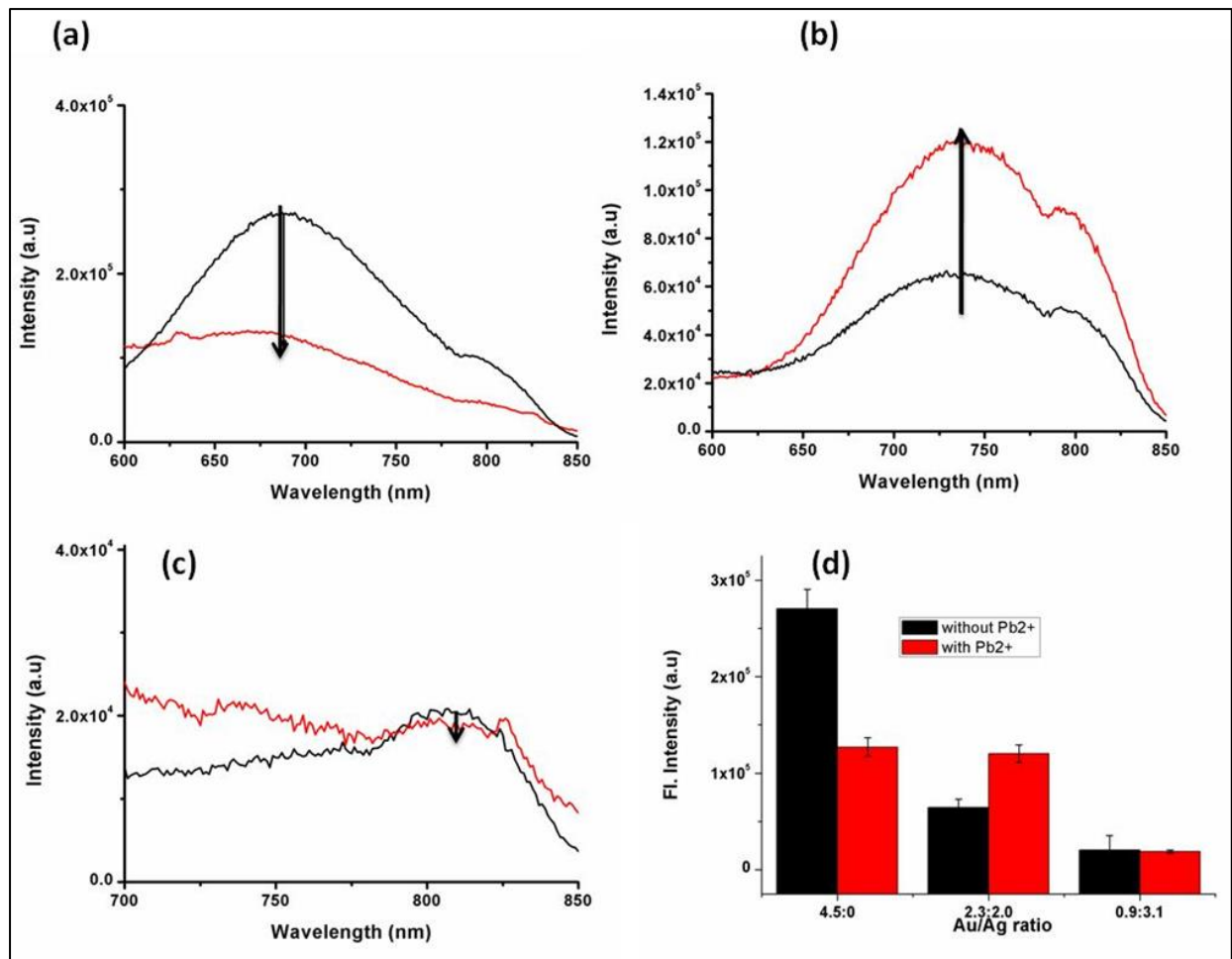


Figure S8. Fluorescence intensity of Au-Ag @BSA NCs containing three different molar ratios of Au/Ag (a) 4.5:0; (b) 2.3:2.0 and (c) 0.9:3.1 in presence(red) and absence of Pb^{2+} (black).(d) plot of fluorescence intensity against three ratio of Au/Ag suggesting the significant enhancement of intensity only for the ratio 2.3:2.0.

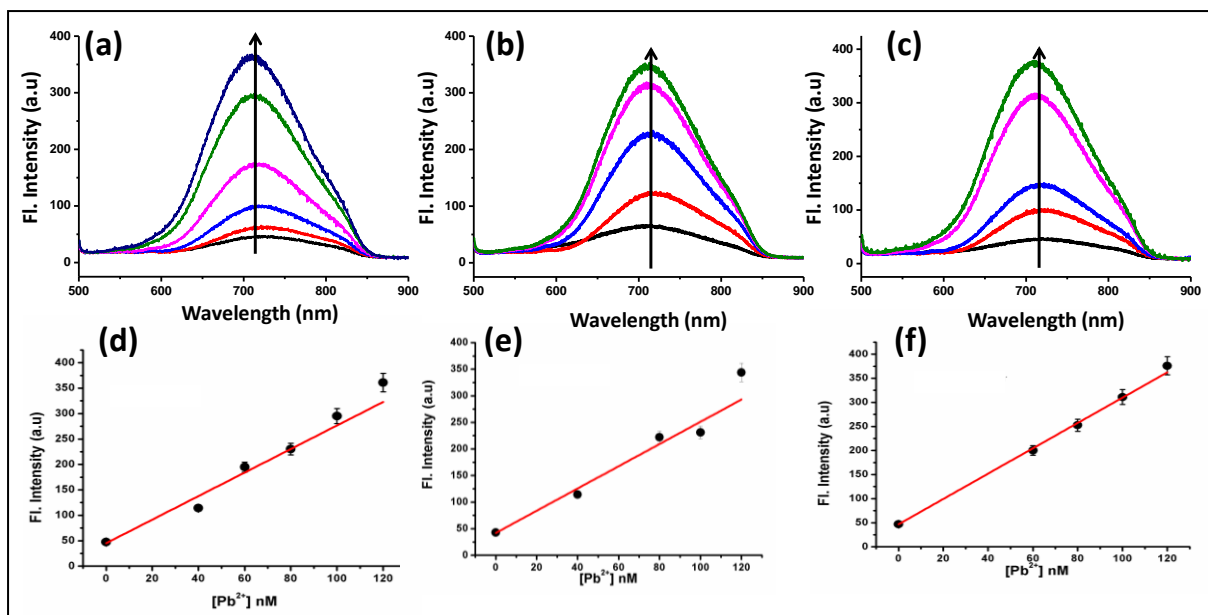


Figure S9. Fluorescence intensity increment of Au-Ag @BSA NCs (Au/Ag = 2.3:2.0) with gradual addition of Pb²⁺ in (a) tap water, (b) pond water and (c) drinking water (obtained by reverse osmosis of the tap water). Concentration dependence plot for the determination of recovery of Au-Ag@BSA NCs in the presence of (d) tap water, (e) pond water and (f) drinking water (obtained by reverse osmosis of the tap water).

References

- Chai, F.; Wang, C.; Wang, T.; Li, L.; Su, Z., Colorimetric Detection of Pb²⁺ Using Glutathione Functionalized Gold Nanoparticles. *ACS Appl. Mater. Interfaces* **2010**, *2*, 1466-1470.
- Wang, Z.; Lee, J. H.; Lu, Y., Label-Free Colorimetric Detection of Lead Ions with a Nanomolar Detection Limit and Tunable Dynamic Range by Using Gold Nanoparticles and DNAzyme. *Adv. Mater.* **2008**, *20*, 3263-3267
- Pu, K.-Y.; Luo, Z.; Li, K.; Xie, J.; Liu, B., Energy Transfer between Conjugated-Oligoelectrolyte-Substituted POSS and Gold Nanocluster for Multicolor Intracellular Detection of Mercury Ion. *J. Phys. Chem. C* **2011**, *115*, 13069-13075.
- Annie Ho, J.-a.; Chang, H.-C.; Su, W.-T., DOPA-Mediated Reduction Allows the Facile Synthesis of Fluorescent Gold Nanoclusters for Use as Sensing Probes for Ferric Ions. *Anal. Chem.* **2012**, *84*, 3246-3253.
- Paramanik, B.; Bhattacharyya, S.; Patra, A., Detection of Hg²⁺ and F⁻ Ions by Using Fluorescence Switching of Quantum Dots in an Au-Cluster-CdTe QD Nanocomposite. *Chem. Eur. J.* **2013**, *19*, 5980-5987.

6. Shi, X.; Gu, W.; Peng, W.; Li, B.; Chen, N.; Zhao, K.; Xian, Y., Sensitive Pb^{2+} Probe Based on the Fluorescence Quenching by Graphene Oxide and Enhancement of the Leaching of Gold Nanoparticles. *ACS Appl. Mater. Interfaces* **2014**, *6*, 2568-2575.
7. Liu, Y.; Ai, K.; Cheng, X.; Huo, L.; Lu, L., Gold-Nanocluster-Based Fluorescent Sensors for Highly Sensitive and Selective Detection of Cyanide in Water. *Adv. Funct. Mater.* **2010**, *20*, 951-956.
8. Zhao, W.; Ge, P.-Y.; Xu, J.-J.; Chen, H.-Y., Catalytic Deposition of Pb on Regenerated Gold Nanofilm Surface and Its Application in Selective Determination of Pb^{2+} . *Langmuir* **2007**, *23*, 8597-8601.
9. Yang, X.; Xu, J.; Tang, X.; Liu, H.; Tian, D., A Novel Electrochemical DNAzyme Sensor for the Amplified Detection of Pb^{2+} Ions. *Chem. Commun.* **2010**, *46*, 3107-3109.
10. Bain, D.; Maity, S.; Pramanik, B.; Patra, A., Core-Size Dependent Fluorescent Gold Nanoclusters and Ultrasensitive Detection of Pb^{2+} Ion. *ACS Sustain. chem. eng.* **2018**, *6*, 2334-2343.